Egypt. J. Chem. **Vol. 66,** No. **SI 13, 939-949** (2023)

Egyptian Journal of Chemistry

http://ejchem.journals.ekb.eg/

Evaluation of bioactivity, antibacterial, and cytotoxicity of the glass ceramic based on akermanite glass containing Ag_2O

[1]Basma Yousef El adawy*; [1]Aida A. Salama; [1]Heba S. Zayed; [2]Mostafa Mabrouk; [3]Esmat M.A. Hamzawy

[1]Faculty of Science, Al-Azhar University (Girls), Nassar City Cairo

[2]Refractories, Ceramics and Building Materials Dept., National Research Centre, 33 El-Buhouth St., Dokki, Cairo 12622, Egypt

[3]Glass Research Dept., National Research Centre, 33 El-Buhouth St., Dokki, Cairo 12622, Egypt

Abstract

Akermanite-based glass ceramics were prepared with /without Ag_2O. Different techniques (DTA, XRD, SEM, and FTIR) are used for the characterization of the synthesized samples. For all prepared glass-ceramic samples, bioactivity, degradation, and ion release were tested in simulated body fluid (SBF). Also, the antibacterial effect was tested with Staphylococcus aureus, Escherichia coli, Klebsiella pneumoniae, and Pseudomonas aeruginosa. Moreover, the cytotoxicity against the normal fibroblast (Wi-38) cell line was studied. DTA shows the addition of Ag_2O lowered the glass transition temperatures to a little extent. the XRD results show that raising the sintering temperature from 900 ˚C to 1000 ˚C led to more crystallinity of Akermanite, cuspidine, and monticellite phases. The microstructure shows submicron crystals in a glassy matrix. After immersion in SBF, nano- and submicron particles of hydroxyapatite were detected in all samples. The integration of silver in the samples enhanced their ability to form hydroxyapatite and increased their antibacterial activity. Cytotoxicity test indicated that all samples up to concentration 125 um/ml had no toxic effect on cells and could be safely used as biocompatible materials.

Keywords: Akermanite based glass ceramic; Ag_2O; bioactivity; antibacterial; cytotoxicity

1. INTRODUCTION

The regeneration of bone defects results from several reasons including necrosis, chronic inflammatory injury, osteoporosis, accidents, trauma, and infections in bone tissue engineering, which is a biomedical challenge worldwide due to the aging population [1]. Some specific compositions of glass ceramics and bioactive glasses have been shown to develop contact with both hard and soft tissues [2]. Dr. Larry L. Hench was the first to discover the bioactive glass. Hench offered the idea that a synthetic material that can produce hydroxyapatite (HA) structure on its surface would be more biocompatible than metals or polymers that the body rejects [3]. Later, this particular glass was known as Bioglass. Silicate-based ceramics and bioactive glass ceramics are widely investigated in the biomedical field [4]. These materials have higher degradation rates and mechanical strengths when compared to phosphate-based bioactive glass ceramics such as hydroxyapatite (HA) [5]. Elements, such as Ca, Mg, and Si, in the glass-ceramics play an important role in the formation of bones in the body [6]. Calcium is the main constituent formation element of the bones and teeth, magnesium is important for regulating bone development, maintenance, and repair, and silicon is also a necessary component that plays an important role in the development of the skeleton [7,8].

Akermanite (Ca2MgSi2O7), a silicate-based bioceramic, exhibits good in vitro bioactivity, mechanical characteristics, and biocompatibility [9]. Akermanite is a type of silicate with the formula Ca2MgSi2O7 that is more commonly used in the field of biomaterials due to its excellent ability to form hydroxyapatite, osteogenesis, and angiogenesis in vivo and in vitro [10,11]. Akermanite (Ca2MgSi2O7) were employed by certain researchers and their findings that after soaking the akermanite in (SBF) for 10 days, hydroxyapatite (HAP) was created. This study showed that akermanite had the ability to generate apatite and might be used to create novel biomaterials which stimulated osteoblasts [12]. Additionally, according to in vivo experiments, akermanite bioceramics significantly

*Corresponding author e-mail basmajoe2012@yahoo.com

Receive Date: 03 March 2023, Revise Date: 01 April 2023, Accept Date: 30 April 2023

DOI: 10.21608/EJCHEM.2023.197674.7671

boosted osteogenesis and angiogenesis in a rat model with a serious calvaria deficiency. where akermanite bioceramics act as prospective biomaterials for osteoporotic bone regeneration due to the effects of Mg and Si ions on osteogenesis, angiogenesis, and osteoclast genesis [11].

Akermanite can be prepared either by dry or wet methods. However, in the current work, akermanite-containing glass was prepared via a melt quenching route [13] due to its ease of milling and low cost for akermanite synthesis, which has greater homogeneity when compared to wet-chemical processes such as sol-gel, precipitation, and hydrothermal [14,15].

Implantation in the human body may be accompanied by the risk of bacterial adherence and colonization on the implant's surface, which may result in implant failure and bacterial infections [16]. Many researchers have studied bioactive glasses doped with silver as an antibacterial to prevent bacterial infections that can lead to implant-associated diseases [17,18]. In this consequence, the use of silver-doped bioactive glass has proven beneficial in preventing bacterial action [19]. However, glasses containing 2 wt % Ag were toxic to cells, whereas those containing 0.75 and 1 wt % are not [20]. Silver's antibacterial activity is well established, and its mechanisms as antimicrobial activities have been proposed in the following points: (1) electron transport interference; (2) binding with the components of the cell; (3) interaction with DNA and causing damage [21]. It has been suggested that incorporating silver ions into the structure of bioactive glass ceramics has improved their bioactivity [17].

The goal of the current study was to create and characterize akermanite using the low-cost raw materials limestone and silica sand. Because akermanite contains more calcium, magnesium, and silicon, it can release more ions, speed up the precipitation of apatite, and thus have higher bioactivity. Calcium fluoride was added to the system as a catalyst, in addition to its antibacterial activity. Furthermore, the silver oxide was added to glass–ceramic in different quantities (0.5 and 1.0) to study the effect of silver doping on morphology, degradation, and SBF bioactivity. Finally, the antibacterial and cytotoxic properties of the prepared samples were also evaluated.

2. Materials and methods

2.1. Materials and preparation of glass-ceramic

The parent glass batch was designed to give an akermanite ($Ca_2MgSi_2O_7$) phase, however, 5% Na_2O was added to lower the melting temperature. The starting materials were limestone (its chemical constituents in wt. % are CaO: 55.70, SiO2: 0.15, Al2O3: 0.22, Fe2O3: 0.02. TiO2: 0.01, MgO: 0.02, Na2O: 0.01, K2O: 0.16 and loss ignition 44.02) silica sand SiO2 (99.4 SiO2, 0.04 CaO, 0.01 K2O, 0.12 Fe2O3, 0.03 SO3), MgCO3 (Fluka Chemika, 98%-Switzerland), CaF2 was added as catalyst (Laboratory Supplies Poole, BHI15ITD, Germany) and Na2CO3 (Fluka Analytical, Sigma-Aldrich, Germany). Silver oxide Ag2O (Spectrum, USA) was added to the base composition, over 100 g glass oxide, in two ratios (0.5 % and 1%). Table 1 shows the chemical compositions of glass samples in terms of oxide weight percentage. Each batch was mixed in an agate ball mill for 5 hours.

Table 1 Glass batch compositions with and without Ag_2O.

Sample code	Chemical Composition Wt %				Additions over 100g glass oxide	
	CaO	MgO	SiO_2	CaF_2	Na_2O	Ag_2O
Ak0	19.04	13.67	40.94	26.50	4.28	-----
AK0.5Ag	19.04	13.67	40.94	26.50	4.28	0.5
AK1.0Ag	19.04	13.67	40.94	26.50	4.28	1.0

The well-admixed homogenized batches were melted in a platinum crucible in the 1350 -1400 °C range range for 2h in a globar furnace. The bubble-free melted glass was poured and quenched in normal distilled (containing little ethyl alcohol) water. The glass frits were dried and then powdered using a ball mill to get glass in the form of powder in grain size < 0.083 mm. The later glass powder was shaped in discs (diameter 1cm) using a stainless mold with uniaxial pressure at 20 KN and a polyvinyl alcohol powder (PVA) 7 % was added as a binder. The shaped discs were separated into two groups, one sintered at 900 ˚C and the other at 1000 ˚C for 2 hours with a heating rate of 10 ˚C /min.

2.2. Characterization

Micro Differential Thermal Analysis (DTA, Shimadzu DTG-60H-Japan) was employed to track the transformation and crystallization temperatures of glass powder (size < 0.35 mm) at a rate of heating (10 ˚C/min). For identification of the formed crystalline phases, x-ray diffraction analysis (XRD, x-ray diffractometer model BRUKER Axs, D8 ADVANCE, Germany) was used. The morphology of the sintered glasses and their elemental microanalysis were investigated with scanning electron microscope coupled with energy-dispersive x-ray microanalysis (SEM/EDX SEM Model Quanta Fei, 250, Holland). Fourier transform infrared spectroscopy (FTIR, JASCO Asia Portal-FT/IR-4600 FTIR Spectrometer) was used to get the functional groups that existed in the samples. The infrared reflection spectra of sintered samples were measured at room temperature (20 ˚C) between 400 and 4000 cm-1 wavenumbers with a resolution of 2 cm-1. A gas Pycnometer was used to determine the real density of the sintered samples. The samples' weight was first determined using a digital balance (4 digits). The gas pycnometer method determines the real density by measuring the sample's real volume. (Upyc 1200e V5.03 Quantachrome Instruments)

2.3. Biodegradation and bioactivity evaluations

The biodegradation and the ability of synthesized glass ceramic to form hydroxyapatite were carried out for the samples that sintered at 1000 ˚C in the simulated body fluid (SBF), prepared according to Kokubo and Takadama [22] and adjusted at pH 7.4 (37°C). For the bioactivity test, the sintered samples were soaked in SBF for 14 and 28 days. Moreover, the degradation process was monitored by the measurement of weight loss according to equation (1) and the pH variation of the SBF solution. The measurement of the variation of calcium, magnesium, and phosphorous ions released from the samples into SBF after different periods was also carried out and analyzed using an inductively coupled plasma optical emission spectrometer (ICP-OES). The formation of the hydroxyapatite layer on the surface of the sintered samples was verified by using SEM, EDX, and FTIR.

Weight loss %= (W0-Wt/W0) X100 (1)

Where W0 is the mass of the sample before immersion on SBF, and W_t is the mass at the immersion time (t).

2.4. Antimicrobial activity

Antimicrobial activity of the prepared sintered akermanite based glass ceramic samples was performed on Gram-positive bacteria (Staphylococcus aureus) and also Gram-negative bacteria (Escherichia coli, Klebsiella pneumoniae, and Pseudomonas aeruginosa) using the agar diffusion method [23]. Several human pathogenic bacteria were employed as the test specimens, according to (Perez et al. (1990). A pure culture of the test specimens was subcultured in nutrient broth, and the strain was then uniformly layered with Muller-Hinton agar on sterile petri plates. Using a sterile cork-borer, a 6 mm diameter circular well was created in plates. There were (100 µl) in the well. The plates were incubated at 37 ºC overnight to test the antibacterial activity, and the zones of inhibition were quantified (positive control was an antibiotic, while the negative control was distilled and sterilised water), [24,25].The tested microorganisms were isolated and identified at the microbiology unit et al.-Azhar University, Cairo, Egypt.

2.5. Cytotoxicity assessment

The cytotoxicity of the prepared samples was determined using normal human lung fibroblasts (Wi 38), by using (MTT protocol) To create a fully formed monolayer sheet, 1×105 cells/ml (100 ul/well) of cells were added to the 96-well tissue culture plate. This was then incubated at 37 °C for 24 hours. Confluent sheets of cells were generated, growth medium was decanted from 96-well microtiter plates, and the cell monolayer was twice washed with wash media (two-fold dilution) prepared in medium with 2% serum (maintenance medium) Three wells served as the control and received only maintenance medium while 0.1 ml of each dilution was tested in the remaining wells. The plate was tested after an incubation period of 37 °C. Cells were examined for any physical toxicity indicators, such as (partial or complete loss of monolayer, rounding, Shrinkage, or cell granulation). Each well received 20ul of MTT solution, which was then well mixed into the medium for 5 minutes on a shaking table at 150 rpm. The media was then incubated (at 37 °C and 5% CO2) for 1–5 hours to allow the MTT to be metabolised. then removed the media, dried the plate if necessary, to get rid of residue, and redissolved the formazan (MTT metabolic product) in 200ul DMSO. The formazan and DMSO were then properly mixed by being shaken table at 150 rpm for five minutes to completely blend the solvent and the formazan. Finally, optical density values were recorded at wavelength 560 nm and subtract background at 620 nm, whose optical density should be directly correlated with cell quantity[26].

2.6. Statistical analyses

All data were presented as means of standard deviation (SD) for n = 3 and analyzed using standard Student's t-test and two-way ANOVA, with Tukey's test for post hoc pairwise comparisons, using the Instant and Prism software package (GraphPadSoftware, Inc., San Diego, CA, USA). The significance level is chosen at $p< 0.05$.

3. Results and discussion

3.1. Characterization of the glass samples

The DTA curves of the prepared glass AK0, and AK1.0Ag (Figure 1), show that the addition of 1%of Ag_2O to the composition of the glass leads to a minor change in each of the softening (endothermic) Ts ˚C and exothermic Tc ˚C temperatures to a lower temperature. The TS temperature was reduced from 600 ˚C in AK0 to 578 ˚C in AK1.0Ag. In the same manner, the TC temperature decreased from 830˚C to 817 ˚C [27]. 'This might be owed to the relative melting point of Ag_2O, wich is about 300ºC. This in turn decreases the metling temperature of the Ag_2O containing samples.

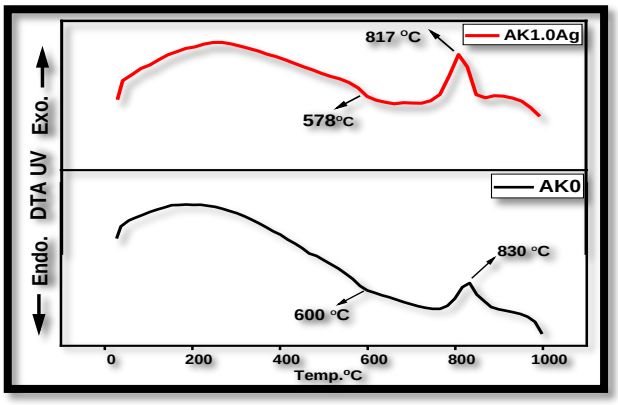

Figure 1: DTA curves of the AK0 and AK1.0Ag glasses.

Figure 2 shows the XRD patterns of the prepared glass samples that sintered at 900 ˚C / 2 hr (Figure 2a) and which sintered at 1000 ˚C /2 hr (Figure 2b). At 900 ˚C /2h, the XRD pattern reveals a clear amorphous glassy matrix containing little phases of akermanite [Ca2Mg(Si2O7), tetragonal, ICDD 87-0052] and cuspidine [Ca4Si2O7(F, OH), ICDD 85-1334]. Raising the sintering temperature to 1000 ˚C/2h led to more crystalline phases of akermanite [Ca2Mg(Si2O7), tetragonal, ICDD 87-0052] and cuspidine [Ca4Si2O7(F, OH), ICDD 85-1334], in addition to the minor appearance of monticellite [CaMgSiO4, orthorhombic, ICDD 84-1325]. As clear from the XRD pattern the incorporation of Ag2O in the prepared samples either at 0.5 or 1% did not cause the development of any additional phases.

The samples that sintered at 1000 ˚C have been approved for later characterization, and their bioactivity, antibacterial effect, and cytotoxicity were evaluated.

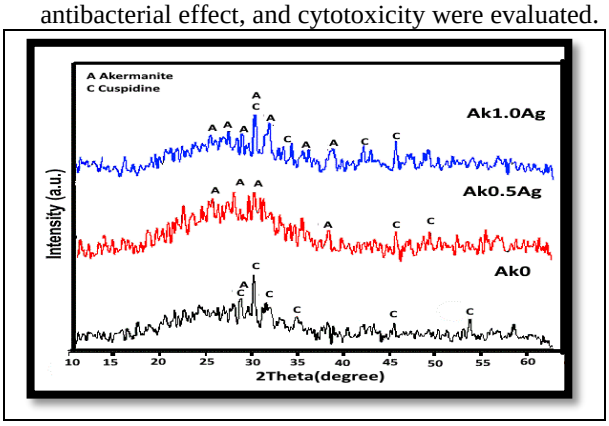

Figure 2(a): X-ray diffraction patterns of the prepared glass heat-treated at 900 ˚C/2h.

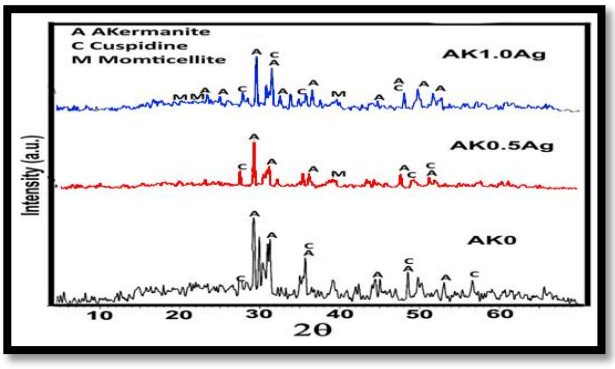

Figure 2(b): X-ray diffraction patterns of the prepared glass heat-treated at 1000 ˚C/2h.

The SEM micrographs and EDX analysis of the prepared Akermanite-based glass ceramic with and without Ag_2O (AK0, AK0.5Ag, and AK1.0Ag) are shown in (Figure 3) The microstructure of the AK0 sample shows irregular particles with clear edges that are shown as either connected or unconnected ridges, and, nano-size wormy-like particles (100-200 nm) between these particles. The micrographs of AK0.5Ag show connected clusters of short interlocked radiated particles with some euhedral crystals in between. On the other hand, clear clusters containing interlocked euhedral crystals and some of which have octahedral marking in AK1.0Ag. Additionally, EDX analysis (Figure 3) shows that all samples displayed the primary peaks of akermanite, which are calcium, magnesium, and silica. Additionally, there is a little appearance of silver peaks in AK0.5Ag and AK1.0Ag.

The FTIR spectrum of the glass ceramic prepared samples (Figure 4), shows O-Ca-O bending mode at 418-423 cm^{-1} [28] and bending O-Mg-O at 469-475 cm^{-1}. The band at 579 cm^{-1} shows the presence of the Ca=O group. The O-Si-O peak was noticed at 683 cm^{-1} which is attributed to normal vibration modes of Si-O in the SiO_4^{-4} group. Other bands at 893 cm^{-1} and 989 cm^{-1} show the Si-O stretching phases [29]. Also, a broad moisture absorption band was noticed at 3422 cm^{-1}. The incorporation of Ag_2O into the akermanite-based glass-ceramic structure did not alter any functional groups.

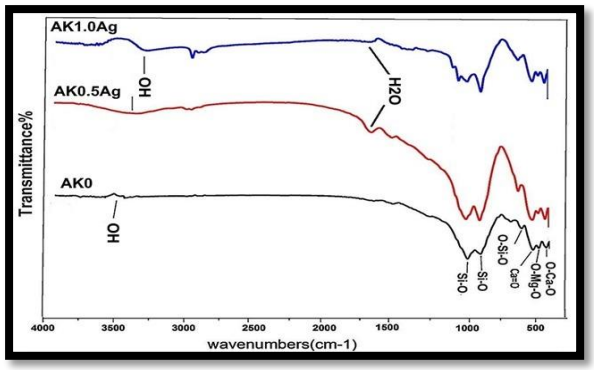

Figure 4: FTIR spectrum for AK0, AK0.5Ag, and AK1.0Ag samples before immersion in SBF

3.2. In vitro, biocompatibility and antibacterial of sintered glasses.

The bioactivity of sintered glasses heat-treated at 1000°C was tested by immersing them in SBF for 2 and 4 weeks. The surface of the produced samples was examined using thin film XRD, SEM/EDX, and FTIR. Studies of degradation and change in densities were also done.

3.2.1. SEM/EDX analysis

SEM micrographs of the surface of the synthesized samples sintered at 1000 °C/2h after soaking in SBF for 14 and 28 days are shown in Figures 5 and 6.

From the figures, it is obvious that all prepared samples have the ability to form hydroxyapatite on their surfaces, and by increasing the immersion time in SBF the surfaces of all examined samples are mostly covered by spherical particles of nanosized or submicron hydroxyapatite. Also, it can be noticed that the incorporation of Ag2O in the samples enhanced their bioactivity either after 2 weeks or 4 weeks in SBF [30,31]

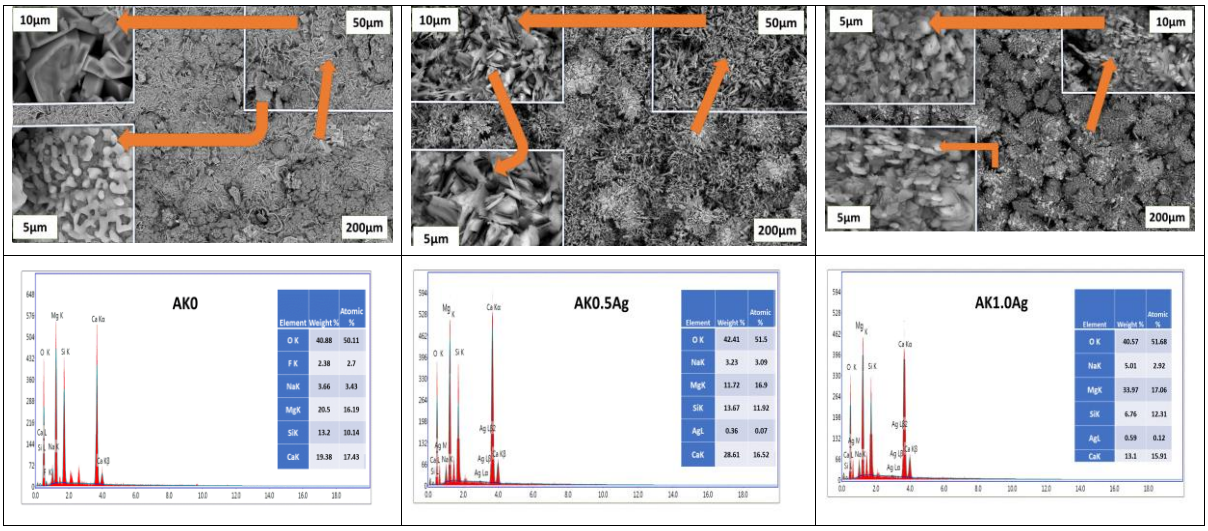

Figure 3: SEM micrographs and EDX microanalysis of AK0, AK0.5Ag and Ak1.0Ag samples.

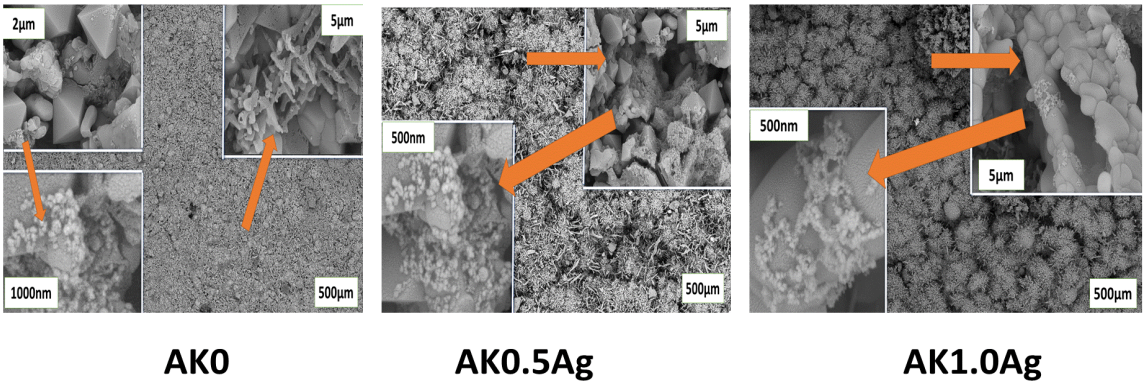

Figure 5: SEM micrographs of AK0, AK0.50 Ag and AK1.00Ag samples soaked in SBF for 2 weeks.

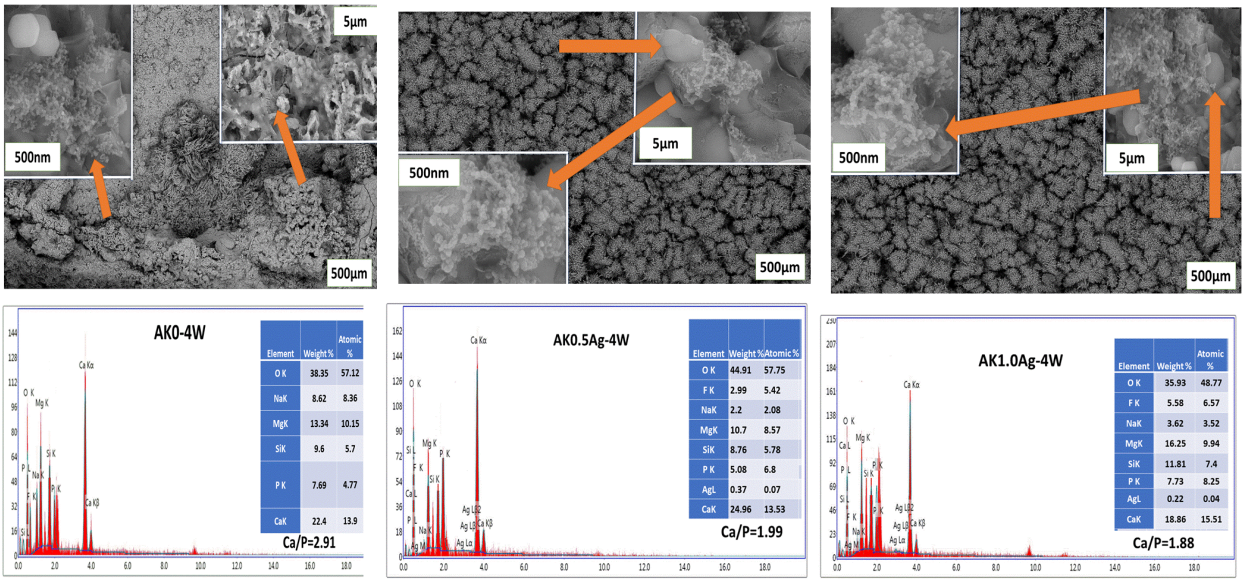

Figure 6: SEM micrographs and EDX microanalysis of AK0, AK0.50 Ag and AK1.00Ag samples soaked in SBF for 4 weeks.

The EDX microanalysis of the sample surface after immersion in SBF shows formation of a phosphate-containing layer [Fig. 6]. The ratios between Ca/P after 4weeks of immersion were 2.91(AK0), 1.99(AK0.50Ag), and 1.88(AK1.00Ag). It is clear that the incorporation of Ag in the parent glass increases the phosphate ratio on the sample surface and enhanced the precipitation of hydroxyapatite on the surface of them. So, the Ca/P ratios are lower for samples containing silver by comparison to that do not. The decrease in this Ca/P ratios makes it closer to the stoichiometric ratio of HAP (1.67).

When the sample is submerged in SBF, the surface starts to produce silanol groups (Si-OH) as a result of the action of Si exchange with H+ from the SBF solution. This group acts as a nucleation location for the calcium phosphate layer that will eventually form hydroxyapatite [32],the incorporation of Ag in the parent glass increases the phosphate ratio on the sample surface which reflects the formation of the hydroxyapatite layer because silver improves their biological activities, silver ions have been known to have strong inhibitory and bactericidal effects. Silver-doped glass and ceramics are expected to be candidates for antibacterial since they show high chemical durability and bioactivity improvement.

2.2. FTIR of the samples after soaking in SBF

Figure 7 shows the FTIR spectrums of AK, AK0.5Ag, and AK1.0Ag glass-ceramic samples after being immersed in SBF for 2 and 4 weeks. The FTIR spectra reflect the production of the HA phase on the surface of all samples post-immersion in SBF. Because hydrolysis of calcium and magnesium occurs in the early stages of bioactivity research, both O-Ca-O and O-Mg-O bands have entirely disappeared in AK0 and have been replaced by the phosphate group. In addition, the relative positions of various functional groups, such as Ca-O, O-Si-O, and Si-O, gradually reduced. The bioactivity after 2 weeks shows bending vibration of phosphate groups that was noticed at 450 - 520 cm^{-1} and 600-610 cm^{-1} while stretching vibration of a phosphate group at 1028 -1089 cm^{-1} is observed on spectra of the samples immersed for 2 weeks and increased at 4 weeks, which indicates the formation of HA layer on the surface of the immersed samples [33]**.** In the case of Ag- containing akermanite samples, a gradual decline in substrate bands and a progressive increment of phosphate band intensity of HA were observed after 2 weeks and completed at the end of four weeks in AK0.50Ag and AK1.0Ag samples [15].

Bending vibration of absorbed H_2O was found at 1644 - 1679 cm^{-1} for all samples in all periods of immersion in SBF and abroad stretching vibration of hydrated OH absorbance peak was found to correspond to 3385 - 34883 cm^{-1} [34,35] (Fig. 7). The substantial growth of more crystalline hydroxyapatite occurred after 14days and continued until the end of four weeks, identifying the soaking duration-dependent behaviour of akermanite.

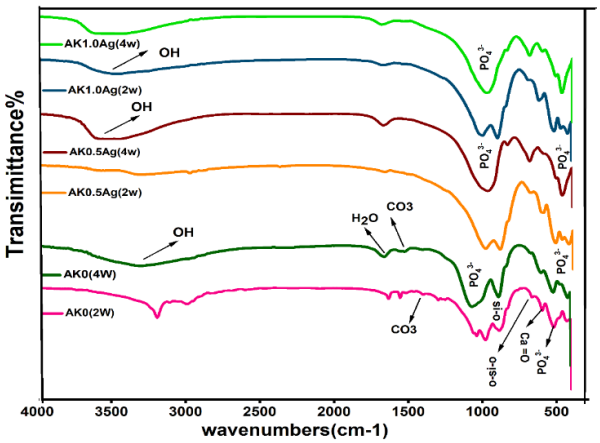

Figure 7: FTIR spectrum for AK0, AK0.5Ag, and AK1.0Ag samples after immersion in SBF for 2 and 4 weeks.

3.2.3. Density measurements

The actual densities of the formed samples using a gas pycnometer are shown in table 2. The actual density of the AK0 before immersion in SBF was 2.511 g /cm^3. The incorporation of Ag_2O to the samples by different concentrations (0.5 % and 1%) possessed slight variation in actual density (2.519 and 2.524g/cm^3) respectively. The actual densities for akermanite-based glass ceramics that were recently measured were more similar to those predicted by earlier studies [36]. Furthermore, the incubation of the prepared samples in SBF for 28 days causes changes to a little extent (2.55, 2.57, and 2.59 g/cm^3) in the values of their actual densities. It is easily noticed that the real densities and their percentage of changes after immersion in SBF for 28 days were increased according to the increase of Ag_2O content in the samples which emphasizes the more precipitation of the hydroxyapatite.

Table.2. Actual densities of the Ak0, AK0.5Ag, and AK1.0Ag samples before and after SBF soaking, along with their percentage of change.

Sample No	Density g/cm^3		
	actual density before soaking in SBF	actual density after soaking in SBF for 28 days	Percentage of actual density change by the time of soaking%
AK0	2.511	2.55	1.55
AK0.5Ag	2.519	2.57	2.024
AK1.0Ag	2.524	2.59	2.614

3.2.4. Degradation studies

The average percentage weight loss observed for AK0, AK0.5Ag and AK1.0Ag samples versus their incubation times in SBF (Figure 8 -a), reveals that all samples had demonstrated a very minor controlled degradation rate (up to 3.8%) in SBF. Recent investigations have developed Ca, Mg, Si-containing

akermanite bioceramics ($Ca_2MgSi_2O_7$), which showed controllable mass loss (%) and accordingly it results in advantageous mechanical properties [14,37]. The same behavior was maintained for all samples during the whole degradation period, but the weight loss % of AK1.0Ag was somewhat higher than those of other two samples. Finally, the weight loss recorded for AK0, AK0.5Ag and AK1.0Ag samples were around 3.59±0.013, 3.77±0.09 and 3.82±0.11 respectively. It is clear that in all samples immediately after immersion in SBF there is a very minor controlled degradation rate. Also, it is obvious that the incorporation of silver in the samples increases to little extent their degradation rate. In all samples, the weight loss increases by time of soaking in SBF, but there is stability at the end of immersion period due to the formation of hydroxyapatite on the surface of all samples.

Furthermore, all of the samples showed the same trend in pH values over the course of the incubation period (Figure 8-b). The pH values of all samples were elevated from 7.44 to around 7.76 on the first day(24hr) of incubation, and then continued to rise to 8.001, 8.050, and 8.09 at the end of the period for AK, AK0.5Ag, and AK1.0Ag, respectively. As a result, the pH values matched the weight loss results (%).

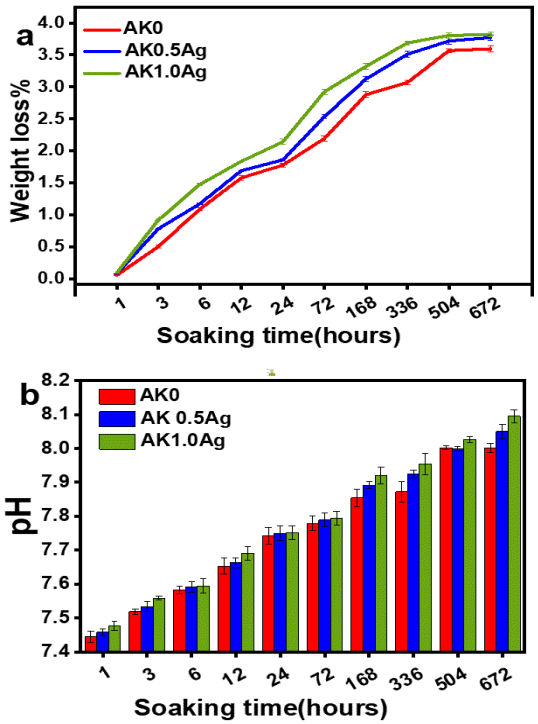

Figure 8: Both a) weight loss (%) and b) pH recorded values of AK, AK0.5Ag and AK1.0Ag samples in SBF at different soaking times.

The released calcium, magnesium, and phosphorous ions were also assessed as indicators of hydroxyapatite production, as shown in Figure 9. The mean calcium ions concentrations released from the samples AK, AK0.5Ag, and AK1.0Ag into SBF solution at various time intervals were observed (Figure 9-a). In which it can be seen that the concentration of Ca^{2+} ions increase fast throughout the first 7 days (168 hr), peaking at 18.19 ±0.05, 17.96 ±0.02, and 17.37 ±0.01 mg/dl for AK, AK0.5Ag, and AK1.0Ag, respectively. Thereafter gradually increases until 21 days (504 hr). After 28 days (672 hr) of immersion, calcium ions concentration decreased to 16.61±0.01, 16.25±.03 and 15.92±.002 mg/dl for AK, AK0.5Ag and AK1.0Ag, respectively, which is an indirect indication for the calcium precipitations onto the surfaces of the materials.

The elevation in ions released in the first 7 days (168 hr), was due to calcium ions exchange with H^+ or H_3O^+ ions into the solution [29]. The following decrease in calcium ion concentration may be attributed to the precipitation of Ca^{+2} ions onto the surface of the bioactive materials due to the attraction of the negative charge of Si-OH groups [38]. On the other hand, the addition of sliver had decreased Ca^{+2} ions release from akermanite samples compared with the behavior of calcium ions release of the pure akermanite. The increase in calcium ions concentration is related to the dissolution of the Ca^{+2} ions from the sintered sample. Therefore, the rapid increase in the calcium content may increase the degree of the apatite layer. Considering the HA formation, the SBF was already supersaturated even before immersion. Therefore, it can be said that the dissolution of the Ca^{+2} ions from the sintered body facilitates the formation of HA [27].

Figure 9-b shows the average value of magnesium ions released from the samples AK, AK0.5Ag and AK1.0Ag into SBF solution at different time periods. It is obvious, that there is a rapid increase in magnesium ions concentration during the first 7 days (168 hr) reaching the highest values of 10.17± 0.03, 10.42±0.06, and 10.37±0.005 mg/dl for AK, AK0.5Ag and AK1.0Ag, respectively. Thereafter, gradually a steady-state was observed for the magnesium release from all the samples for up to 28 days (672 hr) , figure with values of (10.89±0.18), (10.1±0.21) and (10.5±0.13) mg/dl for AK0, AK0.5Ag and AK1.0Ag, this was consistent with early reported work indicating that appetite had covered the surface[39].

Figure 9-c demonstrates how the concentration of SBF phosphorus ions changes over time in different samples. It indicates a quick decrease in the phosphorous ions concentration initially after soaking of all samples, and this decrease reaches its higher degrees by time. This could be due to the utilization of phosphorus in the precipitation of HA layers on the surface of samples [25]. It was well noticed that the decrease in P ions after 21 days (504 hr), and 28 days (672 hr) of incubation was higher in the samples containing silver than the pure akermanite since the P ions were needed for the HA formation. The pH, degradation and ions released in SBF are in agreement with the results obtained by FTIR and SEM imaging after soaking in SBF.

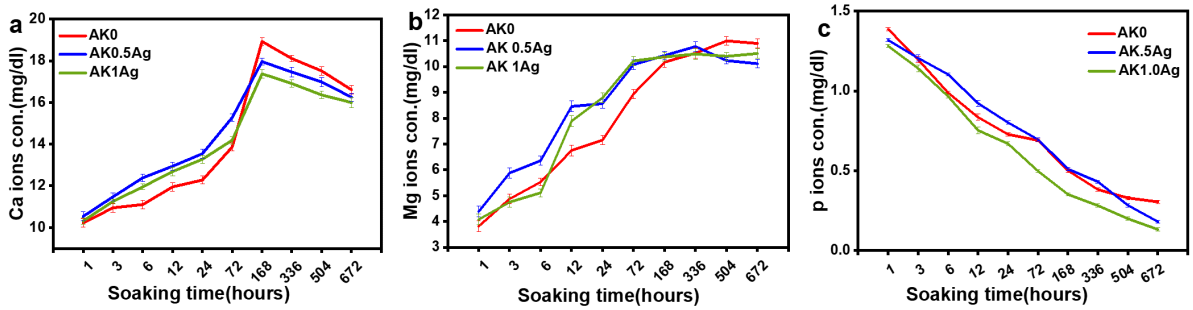

Figure 9: ions released in SBF of a) Ca, b) Mg and P from AK, AK0.5Ag and AK1.0Ag samples at different soaking time.

3.2.5. Antibacterial effect of prepared samples

During this assessment sintered samples were tested for their antibacterial activities. Table 3 and Figure 10(a, b and c) for AK0, AK0.5Ag, and AK1.0Ag respectively illustrate the diameters of inhibition zones formed by synthesized tested samples against examined gram-negative (Escherichia coli, Klebsiellapneumoniae, and Pseudomonas aeruginosa) and gram-positive bacteria (Staphylococcus aureus). As it is obvious, all prepared samples have an inhibitory effect on the activity of all tested species, furthermore, the dopping with silver increased this inhibitory effect. So, the AK1.0Ag sample has almost the biggest inhibition zones for all tested germs [15].

The antibacterial effect of the sintered samples is owed to the liberation of alkaline ions, particularly calcium, and magnesium, that cause an increase in pH of the medium and osmolarity, as a result, cell depolarization occurs, which leads to the death of cells [40]. On the other hand, both gram-positive and -negative bacteria are coated with molecules that have a negative charge, so they have a strong attraction for positive ions released from the sample, leading to intracellular damage [41]. Moreover, glass-ceramic containing silver demonstrated excellent antibacterial properties may be a result of the interaction of the released silver ions with the bacterial membrane that results in membrane disruption and cell death [42]. It is well known that Ag can yield reactive oxygen species (ROS) that interact with the intracellular active components of the cell and cause DNA fragmentation, and damage, and lead to bacterial cell death [43,44].

Table.3. Samples inhibition zone diameter (in millimetres)

	Diameter of inhibition zone (mm)			
Sample No.	**Gram-negative bacteria**			**Gram-positive bacteria**
	Escherichia coli	***Klebsiellapneumoniae***	***Pseudomonas aeruginosa***	***Staphylococcus aureus***
AK0	**11±0.27**	**11±0.36**	**10±0.61**	**11±0.55**
AK0.5Ag	**16±0.53**	**15±0.41**	**18±0.56**	**17±0.36**
AK1.0Ag	**18±0.51**	**17±0.72**	**22±0.26**	**16±0.47**

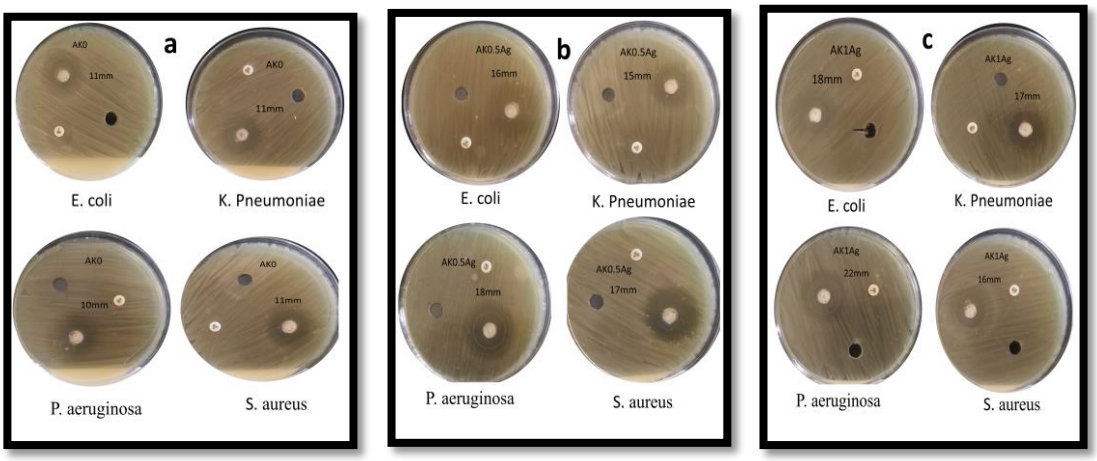

Figure 10: antibacterial tests of a) AK0, b) AK0.5Ag and c) AK1.0Ag against Escherichia coli, Klebsiellapneumoniae, Pseudomonas aeruginosa and Staphylococcus aureus

.

3.2.6. Cytotoxicity effect of prepared samples

To assess the biocompatibility of the prepared sintered samples and the effect of sliver dopping, their cytotoxicity against human lung fibroblast (Wi-38) cells was evaluated by MTT assay. The results of cytotoxicity of samples AK0 and Ak1.0Ag are shown in figure 11 (a, and b). According to the findings (Fig.11, a). At concentrations 31.25, 62.5, and 125 ug/ml, there was no cytotoxic effect for all samples and cell viability was nearly close to 100%.

The viability of the samples drops to 96.87± 0.51 and 91.9±2.12 for AK0 and Ak1Ag samples, respectively, at 250 ug/ml. When the sample concentration is increased to 500 ug/ml, the viability of the samples decreases slightly to 54.09 ±2.63 and, 41.27±3.23, respectively, for AK0 and Ak1Ag samples. As seen in (Fig. 11-a) the highest dosage given to cells (1000 ug/ml) caused significant morbidity in the cells. Finally, the samples' estimated IC50s for AK0 and Ak1Ag were 617.19±4.23 ug/ml and 547.49 ug/ml, respectively. The viability of cells was decreased in a concentration-dependent way.

On the other hand, optical microscope investigations of cell morphology with sample concentrations of 125, 250, 500, and 1000 ug/ml (Fig. 11-b). After 24 hours of incubation, the results revealed that all samples had a low toxicity. The untreated Wi 38 cells were composed of a monolayer of elongated cells in a union monolayer. Wi 38 cells treated with prepared samples showed minimal morphological differences as compared to control cells. After 24 hours of incubation, the number of floating cells in the medium increased, especially at higher concentrations (500 and 1000 ug/ml), and the cells were capable of growing in a monolayer sheet as control cells. As a result, both samples AK0 and AK1Ag were biocompatible and had no harmful effect on cells at concentrations up to 250 ug/ml, and could be safely employed as biocompatible materials for tissue regeneration.

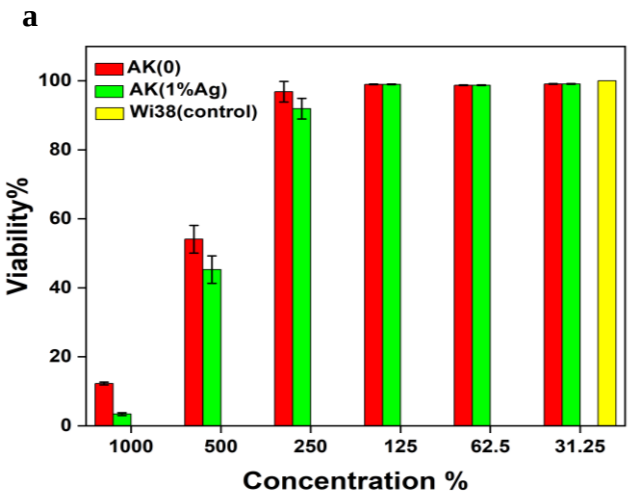

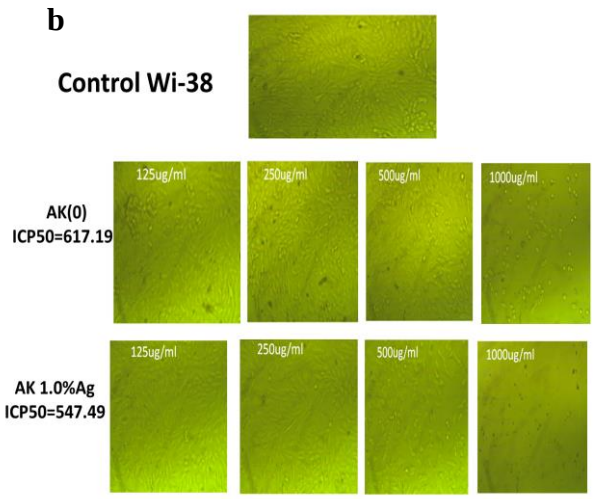

Figure 11: (a)Cell viability % and (b) Morphological features obtained by optical microscope after 24 hours for WI-38 cells treated with samples concentrations (125, 250, 500, and 1000 ug /ml).

4. Conclusions

Akermanite-based glass-ceramics ($Ca_2MgSi_2O_7$) ± Ag_2O were prepared and characterized using DTA, XRD, and SEM/EDX techniques. Akermanite, cuspidine, and little monticellite were developed in the sintered glass samples. The microstructures show submicron and nanoscale grains in addition to clear subhedral crystals. The sintered glasses at 1000 C show good bioactivity and antimicrobial effect and cytocompatibility. The integration of silver in these glass ceramics improved their antibacterial and bioactivity behaviours. Their cytocompatibility test showed equivalent and reasonable cell viability compared to the normal cells.

Acknowledgments

The Authors thank all the help from The Service Laboratories especially the Central Laboratories in the National Research Centre.

Declaration of competing interest

The authors declare that there are no conflicts of interest regarding the publication of this paper.

Funding

The present research did not receive any specific grant from funding agencies in the public, commercial, or not-for-profit sectors.

References

[1] Mohammadi H., Ismail Y.M. B., Shariff k.A., Noor F.M.Assessment of cobalt substitution on the structural, physico-mechanical, and in vitro degradation of akermanite ceramic. J of Science.Advanced Materials and Devices ,2021; 6, 560-8.

[2] Mokhtari S., Krull E. A., Sanders L.M., Coughlan A., Mellott N.P.., Gong Y., Borges R., Wren A.W. Investigating the effect of germanium on the structure of SiO2-ZnO-CaO-SrO-P2O5 glasses and the subsequent influence on glass polyalkenoate cement formation, solubility and bioactivity. Materials Science and Engineering, 2019; C.103: 109843.

[3] Howdhury R. , Cooper L.C. , Shen C. Analysis of Structure, Bioactivity and Hardness of TitaniumIncorporated Bioactive Glass. Biomaterials and Tissue Engineering Bulletin. 2019; 6 ,2393

[4] Sun M., Liu A., Ma C., Shao H., Yu M., Liu Y. Systematic investigation of β-dicalcium silicate-based bone cements in vitro and in vivo in comparison with clinically applied calcium phosphate.cement and Bio-Oss. RSC Advances. 2016 ;6 :586-96.

[5] Mohammadi H., Hafezi M., Nezafati N., Heasarki S., Nadernezhad A., Ghazanfari S. M. H., & Sepantafar M. Bioinorganics in bioactive calcium silicate ceramics for bone tissue repair: bioactivity and biological properties. J. Ceram. Sci. Technol. 2014, 5(1), 1-12.

[6] Choudhary R., Koppala S., Swamiappan S. Bioactivity studies of calcium magnesium silicate prepared from eggshell waste by sol–gel combustion synthesis. J Asian Ceramic Soc. J Asian Ceramic Soc. 2015; 3(2): 173–177.

[7] Demirel M. M, Çanakçi K. and Aydın M. Morphological and antibacterial effects of silver, magnesium, silicon and strontium modified calcium phosphate bone cements prepared by the sol–gel method Advances in Applied Ceramics. 2020; 119:423-33.

[8] Liu W., Wang T. Zhao, X., Dan X. W X. Lu W. , Pan H. Akermanite used as an alkaline biodegradable implants for the treatment of osteoporotic bone defect. Bioact Mater. 2016; 1: 151–9.

[9] Wu C.T. and Chang J.A. novel akermanite bioceramic: preparation and characteristics J. Biomater. Appl. 2006; 21: 119– 29.

[10] Ma V. , Ma B. , Zhou Y. , Zhu H. , Zhou Y. , Huan Z. , Wang Z, Chang P .In vivo evaluation of the subchronic systemic toxicity of akermanite bioceramic for bone regeneration following ISO standard methods.J . RSC Advances. 2019 ; 9 :17530–36.

[11] Xia L., Yin Z., Mao L., Wang X., Liu J., Jiang X., & Fang, B :Akermanite bioceramics promote osteogenesis, angiogenesis and suppress osteoclastogenesis for osteoporotic bone regeneration. Scientific reports. 2016 ;6(1), 1-17.

[12] Wu C., Chang J., Ni S., Wang J: In vitro bioactivity of akermanite ceramics", J Biomed Mater Res. 2005;76A: 73–80.

[13] Naresh P., Srinivas B., Sreenivasu D., Ravikumar D., Nataraju G., Manjari P. S., & Kumar, K. S : Preparation and Characterization of melt derived CaO-Sb2O3-Li2O containing borate glass for multiple application. Journal of Non-Crystalline Solids. 2022; 589, 121642.

[14] Wu C. and Chang J. A review of bioactive silicate ceramics, Biomed. Mater. 2013; 8: 3.

[15] Naresh P., Narsimlu N., Srinivas C., Shareefuddin M., & Kumar K. S: Ag2O doped bioactive glasses: an investigation on the antibacterial, optical, structural and impedance studies. Journal of Non-Crystalline Solids. 2020; 549, 120361.

[16] Simchi A., Tamjid E., Pishbin F., Boccaccin A.R.Recent progress in inorganic and composite coatings with bactericidal capability for orthopedic applications, Nanomedicine. nanotechnology, biology, and medicine. 2011; 7: 22–39.

[17] Bellantone M., Coleman N.J., Hench L.L. Bacteriostatic action of a novel fourcomponent bioactive glass.Journal of biomedical materials research. 2000; 51: 484–90.

[18] Bellantone M., Williams H.D., Hench L.L. Broad-Spectrum Bactericidal Activity of Ag2O-Doped Bioactive Glas"s. Antimicrobial agents and chemotherapy. 2002; 46: 1940– 5.

[19] Blaker J.J, Boccaccini A.R., Nazhat S.N. Thermal Characterizations of Silver containing Bioactive Glass-coated Sutures.Journal of biomaterials applications. 2005; 20: 81-98.

[20] Luo S., Xiao W., Wei X. , Jia C. Z, Huang W. , Jin D. , Rahaman M.N. and Day D.E. In vitro evaluation of cytotoxicity of silver-containing borate bioactive glass.Journal of biomedical materials research part B: Applied biomaterials 2010 ; 95 : 441-8.

[21] Sayed M.R., Neda N., Misaq A., Daryoosh V., Lobat T. Effect of Ion Substitution on Properties of Bioactive Glasses. J.ceramint. 2015; 140: 7241-51.

[22] Kokubo T., & Takadama H. How useful is SBF in predicting in vivo bone bioactivity. Biomaterials. 2006, 27(15), 2907-2915.

[23] Prabhu M., PriscillaS.R, Kavitha Manivasakan K., Rajendran P., Kulandaivelu V . Biomed Res. Int. 2014(2014):10.

[24] Omar A. E., Zayed H. S., & Hamzawy, E. M :Characterization, bioactivity, and antimicrobial activity of CuO-containing devitrite glass–ceramic. Applied Physics A. 2022;128, 1-12.

[25] Mekky, A. E., Farrag, A. A., Hmed, A. A., & Sofy, A. R :Antibacterial and antifungal activity of green-synthesized silver nanoparticles using spinacia oleracea leaves extract. Egyptian Journal of Chemistry. 2021; 64(10), 5781-5792.

[26] Riss T.L., Moravec R.A : Use of multiple assay endpoints to investigate the effects of incubation time, dose of toxin, and plating density in cell- based cytotoxicity assays, Assay and drug development technologies. 2004; 2, 51-62.

[27] Najafinezhad A., Abdellahi M., Ghayour H., Soheily A., Chami A., & Khandan A. A :comparative study on the synthesis mechanism, bioactivity and mechanical properties of three silicate bioceramics. Materials Science and Engineering. 2017; C, 72, 259-267.

[28] Chen L., Zhai D ., Wu C ., Chang J. : Poly(d, l-lactic)-reinforced akermanite bioceramic scaffolds: preparation and characterization Ceram.Int. 2014; 40, 12765–75.

[29] Myat M.H., Ahmad-Fauzi M.N., Masakazu K., & Yanny M.B-I: In vitro Bioactivity of Copper-doped Akermanite Ceramic" Malaysian Journal of Microscopy. 2019; 15, 12936.

[30] Głąb M., Kudłacik-Kramarczyk S., Drabczyk A., Walter J., Kordyka A., Godzierz, M., & Sobczak-Kupiec A: Hydroxyapatite obtained via the wet precipitation method and PVP/PVA matrix as components of polymer-ceramic composites for biomedical applications. Molecules. 2021; 26(14), 4268.

[31] Mobasherpour I., Heshajin, M. S., Kazemzadeh, A., & Zakeri, M. Synthesis of nanocrystalline hydroxyapatite by using precipitation method. Journal of Alloys and Compounds. 2007,430(1-2), 330-333.

[32] Jones J., Gentleman E., Polak J., Elements 3, 393 (2007).

[33] Cerruti M.G. Characterization of bioactive glasses. Effect of the immersion in solutions, that simulate body fluids. Ph.D. thesis, University of Turin, Department of Chemistry IFM, (2004)

[34] SasikumarS., Vijayaraghavan R. Characterization of Bioceramic Calcium Phosphates by Rapid Combustion Synthesis"Journal of materials science and technology. 2010; 26: 1114–

[35] Berzina-Cimdina, L., & Borodajenko, N. Research of calcium phosphates using Fourier transform infrared spectroscopy. Infrared spectroscopy-materials science, engineering and technology. 2012;12(7), 251-263.

[36] Zolko C. (2019). Synthesis and Characterization of Akermanite Ceramic by Mechanical Activation. Graduate Program: Mechanical Engineering, Master Thesis.

[37] Wu C., Chang J., & Xiao Y. (2013). Mesoporous bioactive glasses for drug delivery and bone tissue regeneration. Advanced bioactive inorganic materials for bone regeneration and drug delivery, 1. CRC press , eBook ,2013;p244.

[38] Jones J. R., Gentleman, E., & Polak, J. Bioactive glass scaffolds for bone regeneration. Elements. 2007;3(6), 393-399.

[39] Chengtie W.U, Chang J., Wang J., Ni S., Zhai W. Preparation and characteristics of a calcium magnesium silicate(bredigite) bioactive ceramic Biomaterials 2005; 26:2925–31.

[40] Mubina M. K., Shailajha S., Sankaranarayanan R., & Saranya L: In vitro bioactivity, mechanical behavior and antibacterial properties of mesoporous SiO2-CaO-Na2O-P2O5 nano bioactive glass ceramics. Journal of the Mechanical Behavior of Biomedical Materials Mater. 2019; 100, 103379.

[41] SlavinY.N, Asnis J., HäfeliU.O and Bach H.O . Metal nanoparticles: understanding the mechanisms behind antibacterial activity Journal of nanobiotechnology. 2017; 15: 65.

[42] Yi Y I.X., Zhang J., Zhao I.S., Mei M.L. , Li Q. , Chu C.H. The Antibacterial Mechanism of Silver Nanoparticles and Its Application in Dentistry International journal of nanomedicine. 2020 ; 15: 2555-62.

[43] Le Ouay, B., & Stellacci, F. Antibacterial activity of silver nanoparticles: A surface science insight. Nano today. 2015, 10(3), 339-354.

[44] Farjadian, F., Akbarizadeh, A. R., & Tayebi, L. Synthesis of novel reducing agent for formation of metronidazole-capped silver nanoparticle and evaluating antibacterial efficiency in gram-positive and gram-negative bacteria Heliyon. 2020,6(8), e04747